Geol. Mag. **151** (*4*), *2014, pp. 732–748.* © *Cambridge University Press 2013*
doi:10.1017/S0016756813000794

Torellian (*c*. 640 Ma) metamorphic overprint of Tonian (*c*. 950 Ma) basement in the Caledonides of southwestern Svalbard

JAROSŁAW MAJKA*†, YARON BE'ERI-SHLEVIN‡§, DAVID G. GEE*, JERZY CZERNY¶, DIRK FREI|| & ANNA LADENBERGER**

*Department of Earth Sciences, Uppsala University, Uppsala, Sweden
‡Institute of Earth Sciences, The Hebrew University of Jerusalem, Israel
§Swedish Museum of Natural History, Stockholm, Sweden
¶Department of Mineralogy, Petrography and Geochemistry, AGH – University of Science and Technology, Kraków, Poland
||Department of Earth Sciences, Stellenbosch University, South Africa
**Geological Survey of Sweden, Uppsala, Sweden

(*Received* 31 May 2013; *accepted* 29 August 2013; *first published online* 13 November 2013)

Abstract – Ion microprobe dating in Wedel Jarlsberg Land, southwestern Spitsbergen, provides new evidence of early Neoproterozoic (*c*. 950 Ma) meta-igneous rocks, the Berzeliuseggene Igneous Suite, and late Neoproterozoic (*c*. 640 Ma) amphibolite-facies metamorphism. The older ages are similar to those obtained previously in northwestern Spitsbergen and Nordaustlandet where they are related to the Tonian age Nordaustlandet Orogeny. The younger ages complement those obtained recently from elsewhere in Wedel Jarlsberg Land of Torellian deformation and metamorphism at 640 Ma. The Berzeliuseggene Igneous Suite occurs in gently N-dipping, top-to-the-S-directed thrust sheets on the eastern and western sides of Antoniabreen where it is tectonically intercalated with younger Neoproterozoic sedimentary formations, suggesting that it provided a lower Tonian basement on which upper Tonian to Cryogenian sediments (Deilegga Group) were deposited. They were deformed together during the Torellian Orogeny, prior to deposition of Ediacaran successions (Sofiebogen Group) and overlying Cambro-Ordovician shelf carbonates, and subsequent Caledonian and Cenozoic deformation. The regional importance of the late Neoproterozoic Torellian Orogeny in Svalbard's Southwestern Province and its correlation in time with the Timanian Orogeny in the northern Urals as well as tectonostratigraphic similarities between the Timanides and Pearya (northwestern Ellesmere Island) favour connection of these terranes prior to the opening of the Iapetus Ocean and Caledonian Orogeny.

Keywords: Spitsbergen, zircon dating, Neoproterozoic, magmatism, metamorphism, Caledonian.

1. Introduction

Svalbard's Caledonian bedrock is divisible into three main provinces: Eastern, Northwestern and Southwestern (Fig. 1), separated by major, late Palaeozoic, N-trending faults (Harland, 1997; Gee & Tebenkov, 2004). All three incorporate substantial Precambrian complexes. This paper focuses on the Southwestern Province in Wedel Jarlsberg Land, between Bellsund and Hornsund, where recent research in southwesternmost parts (Larionov *et al*. 2010) has established the presence of a Mesoproterozoic (*c*. 1200 Ma) igneous complex (Eimfjellet) thrust over a Neoproterozoic schist and carbonate succession (Isbjørnhamna Group). Elsewhere in Wedel Jarlsberg Land, thick greenschist-facies metasedimentary successions dominate (Birkenmajer, 1975; Czerny *et al*. 1993) and are separated into two parts by a major unconformity (Birkenmajer, 1975; Bjørnerud, 1990). Recent studies have demonstrated that the deformation and metamorphism beneath the unconformity is of late Cryogenian age (Majka *et al*. 2008). New evidence is presented here of earliest Neoproterozoic igneous rocks overprinted by the above mentioned late Cryogenian Torellian Orogeny. The results have implications for interpretations of the Svalbard Caledonides and reconstructions of this orogen in the High Arctic. In a broader sense, the results presented herein call for reconsideration of existing plate tectonic models for the High Arctic region.

†Author for correspondence: jaroslaw.majka@geo.uu.se

2. Svalbard's Caledonian provinces

The Eastern Province comprises two terranes, Nordaustlandet and West Ny Friesland. The former is influenced by the Tonian (Nordaustlandet) Orogeny, with earliest Neoproterozoic (*c*. 950 Ma) syn- and post-tectonic granites (Gee *et al*. 1995; Johansson *et al*. 2000) intruding uppermost Mesoproterozoic to lowermost Neoproterozoic turbidites. The latter are overlain unconformably (Ohta, 1982; Gee & Tebenkov, 1996) by calc-alkaline volcanites (*c*. 950 Ma; Tebenkov, 1983; Ohta, 1985) and thick Neoproterozoic siliciclastic and carbonate successions,

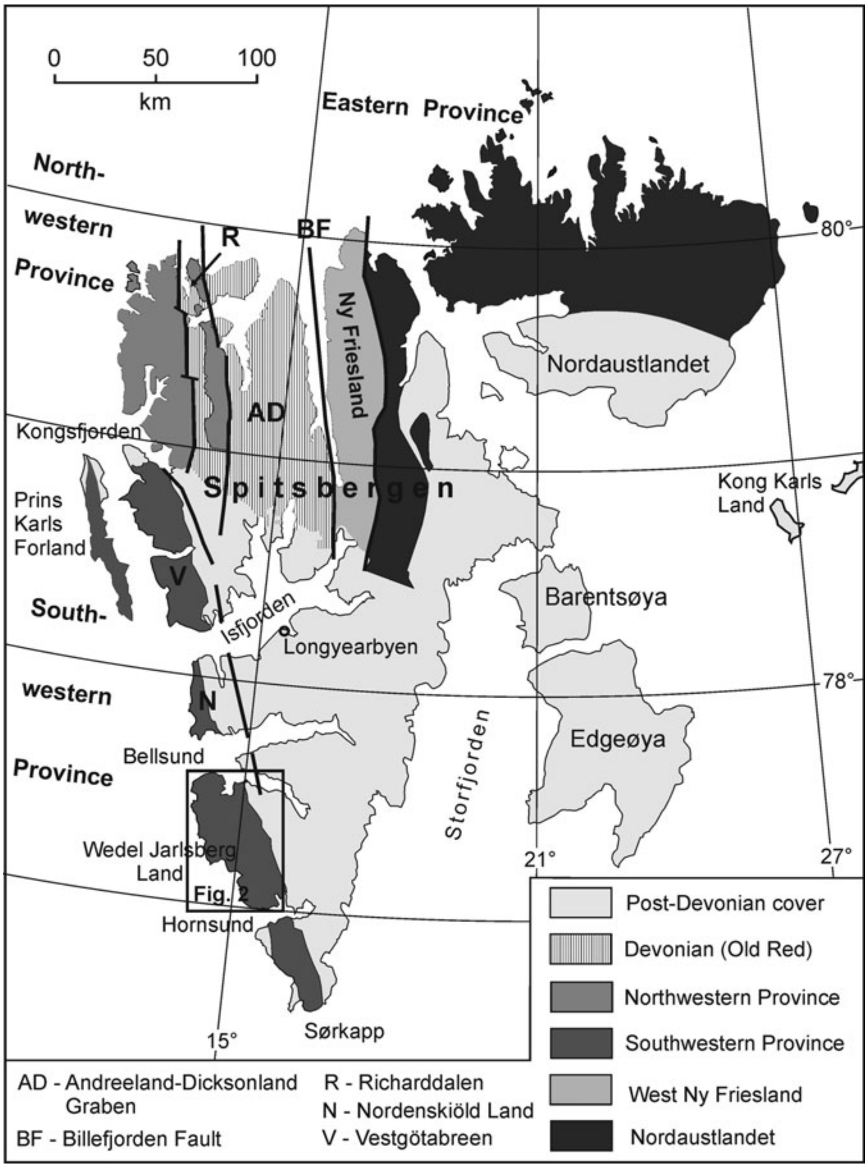

Figure 1. Geological map of Svalbard showing the Caledonian basement provinces (modified from Gee & Tebenkov, 2004).

including Ediacaran tillites that pass conformably up into Cambrian and Ordovician sedimentary rocks. Caledonian migmatization influences the deeper parts of the structural section (Tebenkov *et al*. 2002). By contrast, the West Ny Friesland terrane is dominated by late Palaeoproterozoic (*c*. 1735 Ma) granites (Gee, Björklund & Stølen, 1994; Witt-Nilsson, Gee & Hellman, 1998), locally hosted by late Archaean granitic basement (Hellman, Gee & Witt-Nilsson, 2001), unconformably overlain by, and thrust together with, a Mesoproterozoic metasedimentary cover (Hellman *et al*. 1997) during Caledonian, amphibolite-facies metamorphism. A thrust separates the Nordaustlandet from the West Ny Friesland terrane and, within the latter, there is no evidence of the influence of Tonian tectonothermal activity.

The Northwestern Province, separated from the West Ny Friesland terrane of the Eastern Province by the Andréeland–Dicksonland Old Red Sandstone graben, is also made up of two terranes. Most of this province is similar to the deeper parts of the Nordaustlandet terrane, apparently comprising only upper Mesoproterozoic siliciclastic and carbonate successions that were subject to late Tonian-age deformation and metamorphism, intrusion of *c*. 960 Ma granites (Ohta & Larionov, 1998) and Caledonian migmatization (Gee & Hjelle, 1966; Ohta *et al*. 2002; Myhre, Corfu & Andresen, 2009; Pettersson *et al*. 2009). In one area, east of Raudfjorden, a paragneiss, marble and amphibolite assemblage, the Richarddalen Complex (Group of Gee, 1966), intruded by augen granites (mostly gneisses) and gabbros at *c*. 960 Ma and younger mafic dykes and agmatites at *c*. 660 Ma (Peucat *et al*. 1989), subsequently metamorphosed under eclogite-facies conditions, was intercalated by thrusting with lower grade metasedimentary rocks during the Caledonian Orogeny (Gromet & Gee, 1998).

Svalbard's Southwestern Province is more complex than the others, being located within the Cenozoic belt of transpressive deformation that dominates the

https://doi.org/10.1017/S0016756813000794 Published online by Cambridge University Press

western coast of Spitsbergen, south of Kongsfjorden (Harland, 1997). From northernmost areas near Ny Ålesund (Piepjohn, Thiedig & Manby, 2001), where the rocks deformed during the Caledonian Orogeny occur thrust over upper Palaeozoic and younger strata, to Isfjorden, Bellsund, Hornsund and Sørkapp, the pre-Carboniferous basement is uplifted and incorporated into the core of the West Spitsbergen fold-and-thrust system. The latter flanks the major synform that dominates the structure of southern Spitsbergen (Fig. 1, see also more-detailed geological maps of Svalbard). In southernmost Spitsbergen (Sørkapp Land), Cambro-Ordovician mainly carbonate successions have been described (Major & Winsnes, 1955), with strata of similar age and facies to those on Nordaustlandet. Smith (2000) emphasized correlation of the Palaeozoic strata of Nordaustlandet with Bjørnøya and northeasternmost Greenland. As with the other Caledonian provinces, Proterozoic metasedimentary successions and igneous suites play an important role in the plate tectonic reconstructions; distinguishing their deformation and metamorphism from superimposed Caledonian and younger episodes within the Cenozoic fold-and-thrust belt can be difficult.

In the northern parts of the Southwestern Province north of Isfjorden and including Prins Karls Forland, thick, apparently unfossiliferous, generally low-greenschist-facies metasedimentary formations have poorly defined stratigraphic relations (Harland, 1997) and include thick diamictites, interpreted to be of Ediacaran age and glacial origin (Harland, Hambry & Waddams, 1993). These metasediments comprise the footwall to a thrust sheet that includes greenstones, eclogites and blueschists that yield *c.* 470 Ma K–Ar (Horsfield, 1972) and Ar–Ar (Dallmeyer, Peucat & Ohta, 1990) ages of metamorphism and deformation. These rocks, called the Vestgötabreen Complex (Kanat & Morris, 1988), are unconformably overlain by conglomerates and limestones that pass up into turbidites from which Late Ordovician and early Silurian faunas have been reported (Scrutton, Horsfield & Harland, 1976; Armstrong, Nakrem & Ohta, 1986).

South of Isfjorden, the diamictites reappear at Kapp Linné, where a granite clast has been dated to *c.* 680 Ma using the U–Pb zircon method (Larionov & Tebenkov, 2004). These diamictites are well exposed in a major syncline on the southwestern side of Bellsund (Fig. 2), in northern Wedel Jarlsberg Land (Birkenmajer, 2010; Bjørnerud, 2010), where they overlie a low-grade Neoproterozoic succession that dominates most of the area southwards to Hornsund. Only in the Isbjørnhamna–Eimfjellet area of southwesternmost Wedel Jarlsberg Land, and furthest to the northeast on the ridges to the east and west of Antoniabreen, are more metamorphosed and partly older units preserved.

3. Wedel Jarlsberg Land

The Neoproterozoic successions of Wedel Jarlsberg Land (Fig. 2), underlying the tillites (Kapp Lyell Group) referred to above, are divisible into two main units that have been defined in southern parts as the Sofiebogen and underlying Deilegga groups (Birkenmajer, 1975; Czerny *et al.* 1993). A major discontinuity was recognized to separate these two groups and referred to as the Torellian Unconformity (Birkenmajer, 1975). The Sofiebogen Group is dominated by siliciclastic formations, including basal conglomerates (Slyngfjellet and Konglomeratfjellet formations) with some mafic volcanites, passing up into carbonates and black pelites. The underlying Deilegga Group contains cyclothems of sediments, siliciclastic in lower parts and carbonate-dominated towards the top. In the areas south of Bellsund and beneath the Kapp Lyell tillites, two successions have been described (Bjørnerud, 1990; Dallmann *et al.* 1990), the lower (Deilegga correlative) being referred to as the Nordbukta sequence, and the upper (Sofiebogen correlative) to the Dunderbukta and Recherchebreen 'sequences'. M. Bjørnerud (unpub. Ph.D. thesis, Univ. Wisconsin–Madison, 1987; 1990) and J. C. Nania (unpub. M.Sc. thesis, Univ. Wisconsin–Madison, 1987) have described tight folding and local inversion beneath the Torellian Unconformity separating these units. Detrital monazite, provenance studies (Czerny *et al.* 2010) have yielded ages as young as 950 Ma in the Deilegga Group and 650 Ma in the Sofiebogen Group,

In the vicinity of Hornsund, both on the north and south sides of the fjord, Cambro-Ordovician strata overlie Neoproterozoic successions and are folded and thrust eastwards within the Cenozoic fold belt. Relationships to Devonian Old Red Sandstones further east in the Hornsund area are not well defined.

3.a. Isbjørnhamna–Eimfjellet area

A relatively small part of southern Wedel Jarlsberg Land, located south of Werenskiöldbreen and west of Hansbreen, is separated from the rest of the Wedel Jarlsberg Land basement by a NW-trending, high-angle fault, the Vimsodden–Kosibapasset shear zone. Mazur *et al.* (2009) presented evidence for both dip- and strike-slip movement along this fault-zone and speculated that it may have as much as 600 km of sinistral displacement. To the southwest of the fault, amphibolite-facies metasedimentary and meta-igneous rocks occur in a major, NW-plunging, NE-vergent synform. The suite of meta-igneous rocks, including metagabbros, metagranites, abundant metadolerites and other amphibolites of probable volcanic origin, are underlain and overlain by quartzites with greenschists, mica schists and metarhyolites (Birkenmajer, 1990; Czerny *et al.* 1993) that together compose the Eimfjellet Complex (Group, in previous literature). The overlying quartzites have yielded detrital zircon populations of late Archaean and Palaeoproterozoic age (Majka, Ladenberger & Kuznetsov, 2009), and the gabbros and granites have well-constrained ages of *c.* 1200 Ma (Balashov *et al.* 1995, 1996; Larionov *et al.* 2010).

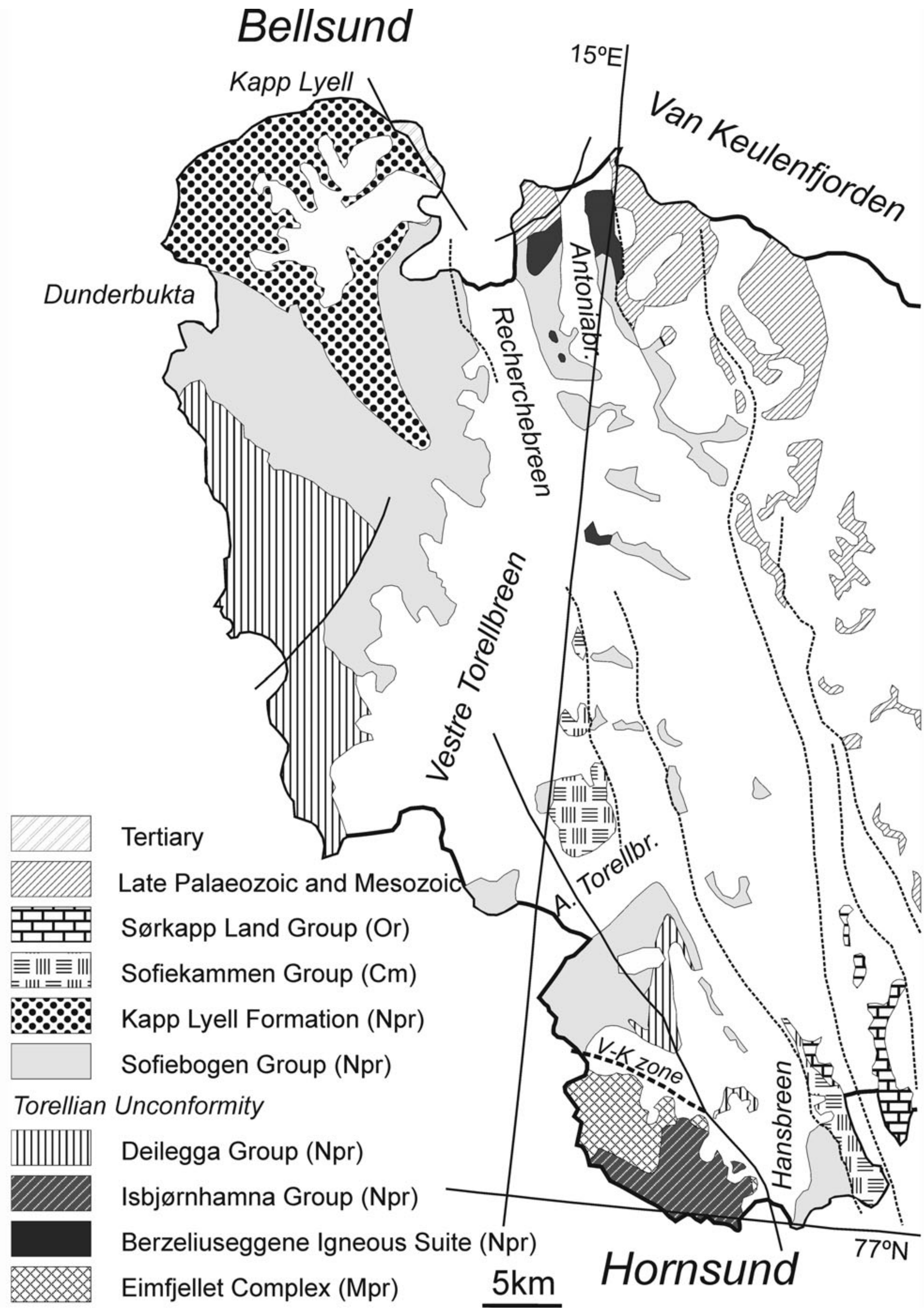

Figure 2. Geological map of Wedel Jarlsberg Land showing the location of the Berzeliuseggene Igneous Suite. V-K – Vimsodden–Kosibapasset shear zone.

https://doi.org/10.1017/S0016756813000794 Published online by Cambridge University Press

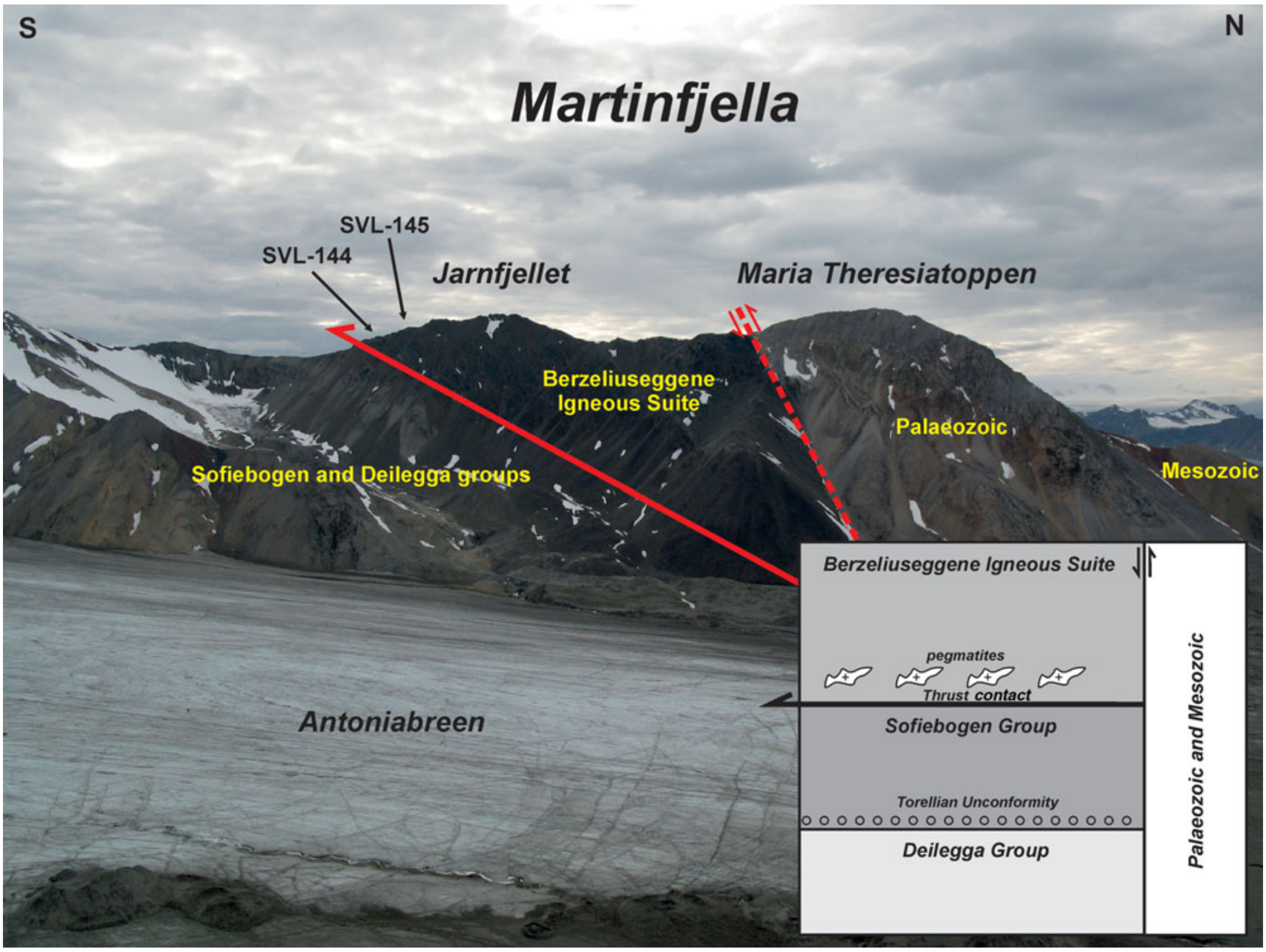

Figure 3. (Colour online) View on the Martinfjella ridge from the east. The Berzeliuseggene Igneous Suite is thrust onto the sedimentary Deilegga (post-950 Ma, Tonian–Cryogenian) and Ediacaran Sofiebogen groups (undivided on the photograph). Locations of the studied samples SVL 144 (77.5072° N, 14.8414° E) and SVL 145 (77.5075° N, 14.8415° E) are indicated by arrows. Inset diagram presents simplified tectonostratigraphy.

The Eimfjellet Complex overlies a thick metasedimentary succession of turbidites and carbonates, the Isbjørnhamna Group, which lack igneous rocks and have yielded detrital zircon populations of mainly Mesoproterozoic age, but including grains as young as *c.* 700 Ma (Larionov *et al.* 2010). Thrust emplacement of the Eimfjellet Complex over the Isbjørnhamna Group and ductile deformation of these metamorphic rocks in southwestern Wedel Jarlsberg Land is probably of Caledonian age, but recent chemical dating of metamorphic monazites (Majka *et al.* 2008) and ion microprobe dating of zircons in pegmatites (Majka *et al.* 2012) have shown the importance of a late Neoproterozoic (*c.* 640 Ma) tectonothermal episode, finding support in previous K–Ar (Gayer *et al.* 1966) and Ar–Ar data (Manecki *et al.* 1998).

3.b. Antoniabreen area

In northeastern Wedel Jarlsberg Land, east of Recherchebreen (Fig. 2), an assemblage of generally greenschist-facies metamorphosed sedimentary and igneous rocks crop out on the ridges along the eastern and western sides of Antoniabreen. They were referred to by E. C. Hauser (unpub. M.Sc. thesis, Univ. Wisconsin–Madison, 1982) as the Antoniabreen sequence and, subsequently, by Dallmann *et al.* (1990) as the Magnethøgda sequence. Within this assemblage of tectonically intercalated units, the higher metamorphosed igneous rocks are represented by augen gneisses (locally gneissic granites, Fig. 3), with some pegmatites, occasional amphibolites and schists, and some very fine-grained igneous rocks, probably of volcanic (rhyolitic and dacitic) origin. The igneous rocks are best developed on the ridge on the east side of Antoniabreen, called Berzeliuseggene, and are therefore referred to here as the Berzeliuseggene Igneous Suite (BIS). The associated metasedimentary units include carbonates (partly dolomitic) and various phyllites and quartzites, and the entire complex is overlain unconformably by lower Carboniferous and younger successions of the south Spitsbergen basin.

On the geological map of Van Keulenfjorden (Dallmann *et al.* 1990), the Magnethøgda sequence is treated as a separate assemblage from the other Precambrian units in the area, perhaps related to the Nordbukta sequence (i.e. Deilegga Group), underlying the Torellian Unconformity. However, these authors drew attention (p. 17) to the possibility that the metasedimentary units in their Magnethøgda sequence

Figure 4. (Colour online) Photograph of the Slyngfjellet conglomerate (marking the Torellian Unconformity) occurring beneath the Berzeliuseggene Igneous Suite basal thrust, located on western slopes of Berzeliuseggene. Hammer for scale is 40 cm long.

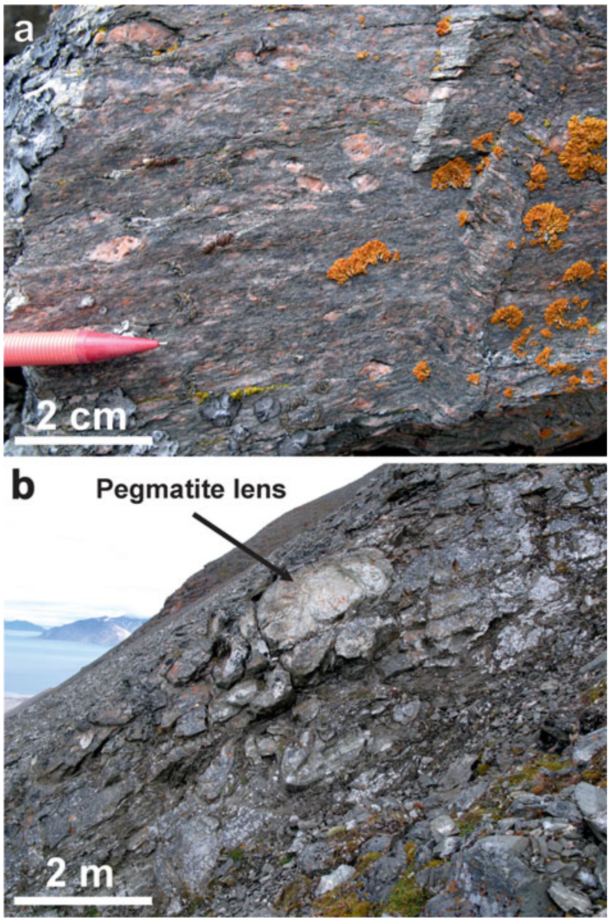

Figure 5. (Colour online) Photographs of sampled and dated (a) augen gneiss and (b) pegmatite of the Berzliuseggene Igneous Suite.

might well be correlated with formations overlying the Torellian Unconformity, including those in the Sofiebogen and Sofiekammen groups. Recent identification of Slyngfjellet-like conglomerates (Fig. 4) overthrust by the BIS, favour this interpretation and suggests the existence of both the Deilegga and Sofiebogen rocks beneath the basal BIS thrust.

The BIS has been described previously as augen gneisses and feldspathic quartzites (Dallman *et al.* 1990 and previous literature) or 'migmatized phyllites' (*sensu* Birkenmajer, 2002); many of the latter are interpreted here to be felsic meta-igneous rocks, and one augen gneiss has been dated in this study, reported below. On the ridge along the eastern side of Antoniabreen, the compositional banding and tectonic contacts with other lithologies dip at low to moderate (30°) angles northwards. The whole succession is tectonically repeated and two different thrust sheets, separated by strongly deformed metasediments of unknown origin, can be observed on Aldegondaberget and Berzeliuseggene. West of Antoniabreen, on Jarnfjellet, only one thrust sheet occurs (see also Fig. 3). Mylonitic and cataclastic varieties of the BIS are ubiquitous, occasionally with visible pseudotachylites. Parageneses in the augen gneisses are generally dominated by quartz (35–40 %), plagioclase (15 %), potash feldspar (8–10 %) and micas (10–20 %). Although extensively retrogressed, the occasional presence of garnet in the BIS indicates earlier amphibolite-facies metamorphism, prior to thrust intercalation with the younger sedimentary rocks. Protoliths of granitic rocks have been identified in the gneisses on the slope northeast of the glacier front. Pegmatites (also analysed in this study) appear to be concentrated towards the base of thrust sheet. Rare schists are also intercalated with the other BIS lithologies.

The BIS was subjected to extensive fluid alteration. Metasomatic zoning patterns are observed to be related to the sole thrust. At the bottom of the sequence, a zone up to a few metres thick of whitish K-feldspar-enriched rocks is present and is overlain by a wider zone of similar, but pinkish K-feldspar-enriched rocks. Earliest K-metasomatism was probably syn-tectonic and developed during thrusting, because the metasomatized rocks form horizons parallel to the thrust sole. However, a later metasomatic stage is the youngest feature in the studied sequence (BIS), because it mostly develops along fractures that cross-cut the main foliation and also commonly overprints the main foliation.

4. New studies of the Berzeliuseggene Igneous Suite

Of the samples from the BIS collected for analytical studies, two have been selected for isotope dating: a fine-grained augen gneiss (SVL 145, Fig. 5a) and a pegmatite (SVL 144, Fig. 5b). Zircons were separated from both samples. One of the samples (SVL 145) was initially analysed (by D.F.) by laser ablation inductively coupled plasma mass spectrometry (LA-ICP-MS) and both were subsequently analysed by ion microprobe (by Y.B.S.) at the Nordsim facility in Stockholm.

4.a. Sample description

4.a.1. Augen gneiss (SVL 145)

The sample was collected on the Jarnfjellet ridge, west of Antoniabreen (Fig. 3). The rock is greyish pink, fine grained and strongly sheared (Fig. 5a). The foliation is defined by a parallel arrangement of muscovite, biotite and quartz-dominated layers. In the latter, subordinate K-feldspar and plagioclase also occur. K-feldspar also forms augen up to 0.5 cm in diameter. Rarely, bigger quartz porphyroclasts are also found. Garnet is quite common and usually forms non-coaxially deformed porphyroclasts aligned in the foliation planes. The metamorphic origin of the garnet is indicated by snowball-like microtextures and its chemistry. Accessory mineral phases in the rock include allanite, titanite and zircon. Allanite is common and is almost always overgrown by later epidote. Rarer titanite is always deformed. Zircon is a very common phase and forms idiomorphic crystals. The intensity of deformation of this felsic rock has thoroughly overprinted its original plutonic or volcanic textures.

4.a.2. Pegmatite (SVL 144)

The sample was also collected on the ridge of Jarnfjellet close to the basal thrust contact of the BIS (Fig. 3). A lens-shaped pegmatite in the host augen gneiss is whitish (Fig. 5b) and coarse grained with quartz, plagioclase, less prominent K-feldspar and muscovite dominating. Quartz exhibits undulatory extinction. Plagioclase is strongly altered and replaced by fine-grained muscovite. By contrast, K-feldspar is rather well preserved. Muscovite usually forms relatively small ($\leq$ 100 μm) matrix flakes; however, bigger ones also occur, occasionally in the garnet pressure shadows. Garnet is rather scarce and forms subhedral slightly deformed crystals. Among the accessory phases, rare apatite, allanite, titanite and zircon were found. Although zircon is not a very common phase, it occasionally forms even macroscopically visible (up to 1 cm long) crystals.

4.b. Zircon separation

Zircon separation was performed by standard methods using a water-table and without heavy liquids, and the grains were handpicked and mounted in a resin disc along with a zircon standard and polished to reveal the grain interiors. The mounts were gold-coated and imaged with a Hitachi S-4300 scanning electron microscope and Gatan mini-CL at the Swedish Museum of Natural History.

4.c. LA-SF-ICP-MS analyses

All U–Pb age data obtained at the Geological Survey of Denmark and Greenland in Copenhagen were acquired by laser ablation single collector magnetic sectorfield inductively coupled plasma mass spectrometry (LA-SF-ICP-MS) employing a Thermo Finnigan Element2 mass spectrometer coupled to a NewWave UP213 laser ablation system. All age data presented here were obtained by single spot analyses with a spot diameter of 30 μm and a crater depth of approximately 15–20 μm. The methods employed for analysis and data processing are described in detail by Gerdes & Zeh (2006) and Frei & Gerdes (2009). For quality control, the Plešovice (Sláma *et al*. 2008) and M127 (Nasdala *et al*. 2008; Mattinson, 2010) zircon reference materials were analysed, and the results were consistently in excellent agreement with the published isotope dilution thermal ionization mass spectrometry (ID-TIMS) ages. Full analytical details and the results for all quality control materials analysed are reported in Table S1 (online Supplementary Material available at http://journals.cambridge.org/geo).

4.d. SIMS analyses

The U–Th–Pb zircon analyses were performed on the Nordsim Cameca IMS-1270 ion microprobe, following methods described by Whitehouse, Kamber & Moorbath (1999) using a spot size of *c*.10–25 μm. Analyses used 12 scans per mass and U/Pb ratio calibration was based on analyses of the Geostandards zircon 91500 (Wiedenbeck *et al*. 1995). Data reduction employed in-house Excel macros. Age calculations were made using Isoplot version 3.02 (Ludwig, 2003). Decay constants follow the recommendations of Steiger & Jäger (1977). Common lead corrections were applied using a modern-day average terrestrial common Pb composition, i.e. $^{207}Pb/^{206}Pb = 0.83$ (Stacey & Kramers, 1975), where significant ^{204}Pb counts were recorded and which are assumed to represent surface contamination. All age errors quoted in the text are 2σ.

4.e. Zircons, isotope data and interpretations

4.e.1. Augen gneiss (SVL 145)

Zircons from SVL 145 are medium sized (100–200 μm) euhedral clear grains of yellowish colour with minor inclusions. Under cathodoluminescence (CL), the zircons exhibit oscillatory to sector zoned cores passing outwards into darker inner rims where only relict oscillatory zoning can be seen. These cores and inner rims are in turn rimmed by bright CL rims, which are best developed at the long terminations of grains where they reach a thickness of up to *c*. 50 μm (Fig. 6; grains 3, 7, 13). The border between the CL-bright

https://doi.org/10.1017/S0016756813000794 Published online by Cambridge University Press

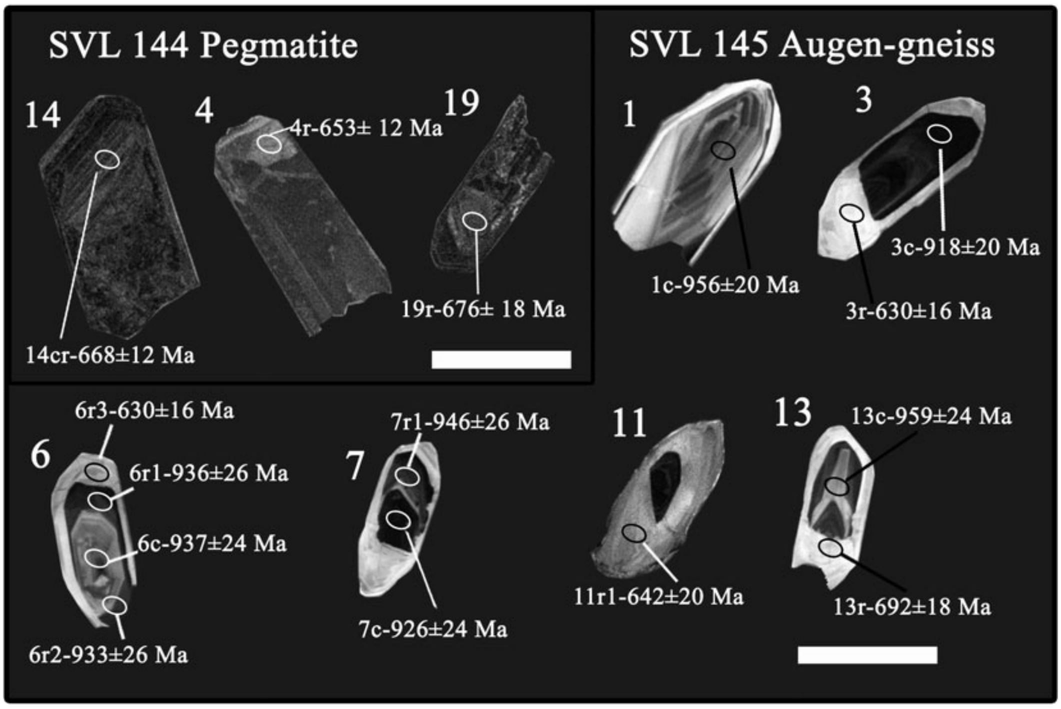

Figure 6. Cathodoluminescence (CL) images of representative zircons from pegmatite sample SVL 144 and augen gneiss sample SVL 145. Ellipses show ion microprobe U–Pb analyses numbered as in Table 1. U–Pb dates are ^{206}Pb–^{238}U ages except for grain 19 of sample SVL 144 where this is ^{207}Pb–^{206}Pb. All dates are quoted with 2σ uncertainties. Horizontal scale bars are 100 μm.

outer rims and the darker inner parts is generally sharp, cross-cutting the internal zoning. However, in a few cases, the internal zoning can be traced out into the CL-bright rims (Fig. 6; grains 7, 13).

The initial analysis of this sample by LA-ICP-MS yielded a concentration of ages (*c*. 85 %) at *c*. 965 Ma, with a trail of apparently younger grains down to *c*. 650 Ma and a few (*c*. 5 %) older analyses at 1100–1200 Ma, 1300 Ma and 1400 Ma, and 1650–1750 Ma (Figs S1, S2 in online Supplementary Material available at http://journals.cambridge.org/geo). Closer examination of the analysed sites with CL images showed that the post-950 Ma ages were from locations within the inner and outer rims, and that the pre-950 Ma ages were all from the cores of the crystals, apparently from xenocrysts. All the analytical data are presented in Table S2 (online Supplementary Material available at http://journals.cambridge.org/geo). Since CL images of the grains indicate a complex zircon growth/recrystallization, interpretation of the LA-ICP-MS analyses is complicated by the possible mixing of domains within an analysis spot. While analyses where spot location was found to have overlapped two zircon domains were omitted from the dataset, possible mixing at the depth of a few micrometres could not be precluded. We therefore chose to apply further secondary ion mass spectrometry (SIMS) U–Pb analyses to zircons from this sample as the shallower analysis spot using this technique is associated with a higher certainty that U–Pb isotope data from two different domains was not mixed.

Thirty-one new SIMS analyses were made on SVL 145 zircons. Twenty-one analyses of oscillatory zoned cores and darker inner rim domains yielded a concordia age of 950 ± 5 Ma (MSWD = 1.3; Fig. S2 in online Supplementary Material available at http://journals.cambridge.org/geo). The darker inner rims exhibit a low range of Th/U (0.02–0.1 average 0.22) relative to the brighter outer domains (0.36–0.89 average 0.63) and thus potentially may reflect post-crystallization Pb-loss events. Nevertheless, no correlation between age and texture was observed. The concordia age is thus interpreted as the best estimate for crystallization of the magma and there is no evident Pb loss in the core–inner rim domains. An additional analysis of an oscillatory zoned core yielded a slightly discordant analysis with a ^{207}Pb–^{206}Pb age of 1341 ± 26 Ma (2σ), and this domain is interpreted as a xenocryst (Fig. 7). This interpretation is supported by the fact that this domain is concordantly mantled by a dark inner rim which yielded a concordant age at *c*. 950 Ma.

Compared with the core–inner rim domains, the bright CL rims are characterized by lower U (35–70 ppm), Th (0–1 ppm) and Pb (4–9 ppm) contents, and by very low Th/U ratios (0.003–0.02). The nature of the contact between the bright CL rims and the inner domains, the low U and Th contents with very low Th/U ratios, as well as the faint oscillatory zoning and shape of crystal faces (both of which are concordant with inner domain oscillatory zoning), are all compatible with fluid-associated recrystallization of the zircon crystal lattice (Corfu *et al*. 2003; Martin *et al*. 2008). Of the ten analyses of CL-bright domains, three yielded a concordia age of 635 ± 10 Ma (MSWD = 0.86; Fig. 7) interpreted to reflect sub-solidus reactions along zircon margins. This fluid-associated process was characterized

https://doi.org/10.1017/S0016756813000794 Published online by Cambridge University Press

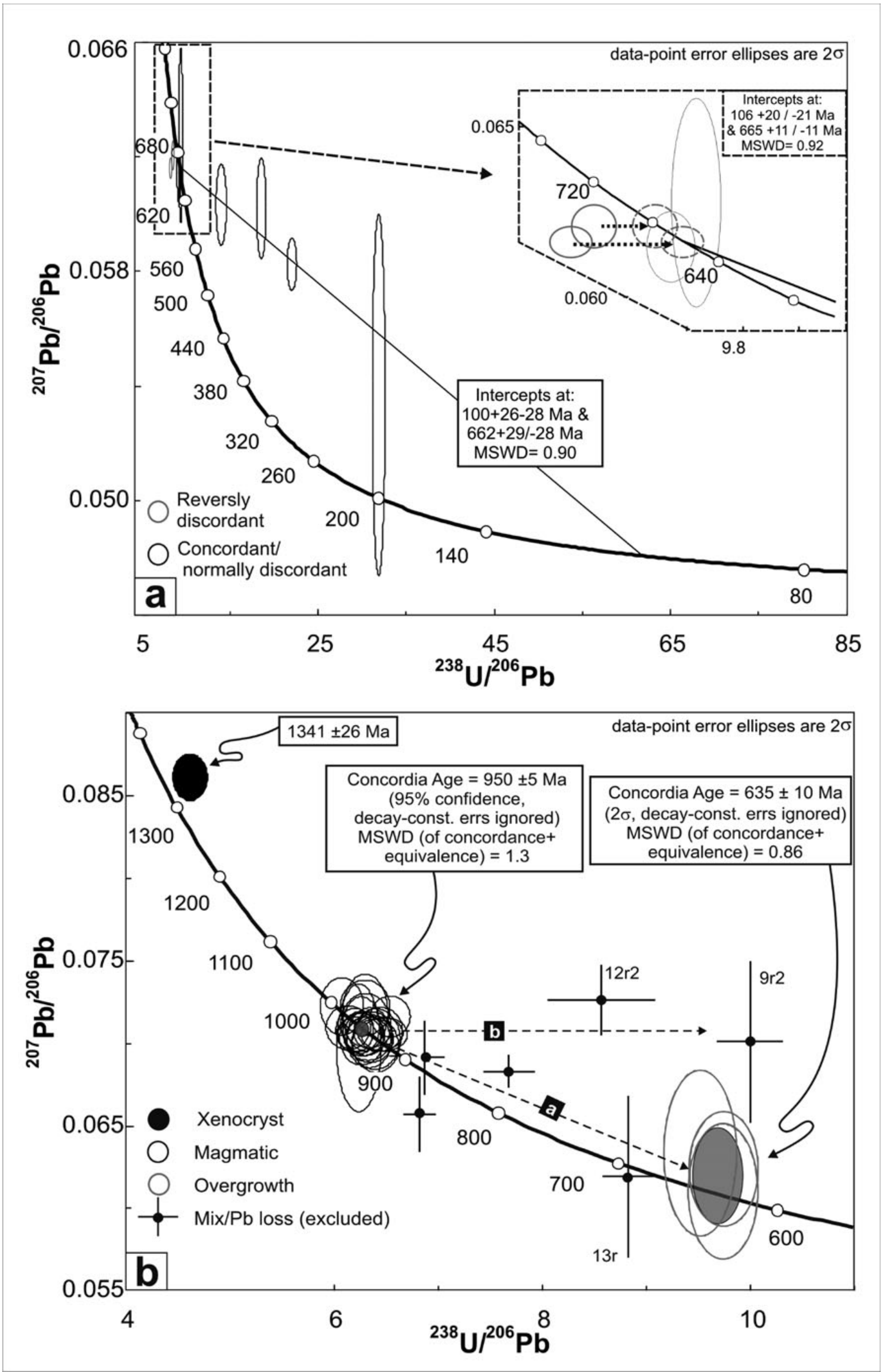

Figure 7. Tera-Wasserburg Concordia diagrams showing zircon ages for the pegmatite sample SVL 144 (a), and augen gneiss sample SVL 145 (b). Inset in (a) shows a discordia line intercept calculation which follows a forced horizontal shift of analyses 19cr and 25cr from their original reversely discordant location onto the concordia. Dashed lines 'a' and 'b' in (b) represent core–inner rim + CL-bright domain mixtures and Pb-loss trends, respectively.

https://doi.org/10.1017/S0016756813000794 Published online by Cambridge University Press

by a reaction front moving inwards into the zircon cores. Post-analytical inspection of several other analytical sites in the CL-bright rims provided evidence that they represented mixtures with core–inner rim domains (Fig. 7; trend line a). This is also reflected by elevated U, Th and Pb and higher Th/U ratios (Table 1). In other cases, analyses are either significantly discordant (Fig. 7; grains 9r2, 12r2) or the age is significantly older than 635 Ma (Fig. 7; 13r), but the post-analytical inspection showed that spots were correctly sited within the CL-bright domains, as is also reflected by low U, Th, Pb and Th/U. The significance of the discordant analyses is difficult to assess, and analyses 9r2 and 12r2 may possibly reflect Pb-loss events associated with zircon recrystallization processes (Fig. 7; trend line b), or problems associated with the common Pb correction for these very low Pb analyses. Analysis 13r is more problematic as it is concordant with a $^{206}Pb–^{238}U$ age of 692 ± 9 Ma (2σ; Table 1). This is interpreted to reflect incomplete recrystallization of the zircon domain with an inherent older age component; however, possible early crystallization pre-dating 635 Ma cannot be ruled out.

4.e.2. Pegmatite (SVL 144)

Zircons from SVL 144 are dominantly medium sized (100–200 μm) euhedral turbid grains containing many small inclusions of unidentified character. Under CL, the grains are generally dark and have little discernable internal structure (Fig. 6), making the dating of these grains challenging. Twenty-two analyses were sited on domains exhibiting faint oscillatory zoning. Two have medium U contents (*c*. 800 ppm) and the rest are characterized by high U concentrations (2000–9000 ppm), which likely resulted in radiation damage, metamict domains, lack of CL response and high common Pb. Indeed, most analyses are associated with high common Pb and low $^{206}Pb/^{204}Pb$ ratios (Table S2 in online Supplementary Material available at http://journals.cambridge.org/geo), and are not further discussed here. Only eight grains with low common Pb are plotted on the concordia diagram (Fig. 7). Six analyses define a discordia line with intercepts at 662 +29/−28 Ma and 100 +26/−28 Ma (MSWD = 0.9), which are interpreted to reflect late Cryogenian crystallization (*c*. 660 Ma) and later Pb loss, probably associated with Cretaceous (*c*. 100 Ma) tectonothermal activity. Two other reversely discordant (7–12 %) analyses were not used for this regression; however, their $^{207}Pb–^{206}Pb$ ages are within error of the upper intercept. If these two analyses are 'forced' horizontally onto the concordia and the age is recalculated using all eight analyses, an age with smaller error is obtained, with intercepts of 665 + 11/−11 Ma and 106 +20/−21 Ma, respectively, as well as a better MSWD of 0.92 (Fig. 7, inset). While the forced shift of the two analyses onto concordia is speculative, it may be justified. Reverse discordance within high-U zircons is considered to reflect problems with the U–Pb calibration between a low-U standard and high-U sample (McLaren, Fitzgerald & Williams, 1994; Wiedenbeck, 1995). Consequently, the location to the left of the concordia may reflect an analytical problem rather than a geologically significant process. We thus consider the discordia intercepts calculated using the combined eight analyses to be a robust estimate of the time of crystallization and the later Pb-loss events.

5. Discussion

The discussion that follows below considers the new isotope age data from Wedel Jarlsberg Land in relation to other evidence from Svalbard. It then examines the relationships between Svalbard's Southwestern Province and the evidence for Neoproterozoic orogeny in northern Ellesmere Island (Pearya) and in the Timanides of northeastern Baltica.

5.a. Mesoproterozoic and late Palaeoproterozoic xenocrysts

The LA-ICP-MS ages of 1100–1200 Ma, 1300–1400 Ma and 1650–1750 Ma in combination with the ion microprobe identification of the presence of 1350 Ma xenocrysts in sample SVL 145, suggest that the BIS magmatic rocks were generated by melting of rocks with Grenvillian signatures. Similar ages have also been recorded in the metasedimentary rocks of northwestern Spitsbergen (Montblanc Formation) and associated migmatites (Ohta, Larionov & Tebenkov, 2003) and from the Krossfjorden Group metasediments (Pettersson, Pease & Frei, 2009). The 1350 Ma ages, in particular, have been compared with the Metamec Complex and Nain Plutonic Suite of the Eastern Grenville Province (Pettersson Pease & Frei, 2009). Ages of *c*. 940 Ma and *c*. 1360 Ma were also obtained on xenocrystic zircons from Frænkelryggen tuffites interbedded with Devonian Red Bay Group sandstones occurring within the Raudfjorden graben in northwestern Spitsbergen (Hellman *et al*. 1997).

5.b. Early Tonian magmatism in southern Svalbard

The dating here of the BIS augen gneiss sample (SVL 145), indicating magma crystallization at 950 ± 5 Ma, provides the first unequivocal evidence of early Tonian igneous activity in southwestern Spitsbergen. Previous isotope age investigations of magmatic rocks in Wedel Jarlsberg Land have identified *c*. 1200 Ma Ectasian–Stenian plutonic and volcanic rocks in the Eimfjellet Complex (Larionov *et al*. 2010), with no record of younger Tonian rocks. Magmatism of this age has been previously reported from both Svalbard's Eastern and Northwestern provinces. In Nordaustlandet, the *c*. 970–940 Ma ages include both granites, and andesites and rhyolites (Gee *et al*. 1995; Johansson *et al*. 2005). In the Northwestern Province, granites (usually augen gneisses) and gabbros yielded *c*. 960 Ma ages (Peucat *et al*. 1989; Ohta & Larionov, 1998; Pettersson, Pease & Frei, 2009). Recently, Gasser & Andresen (2013) have reported a *c*. 930 Ma augen gneiss of unknown

https://doi.org/10.1017/S0016756813000794 Published online by Cambridge University Press

Table 1. SIMS U–Th–Pb data

							Ratios								Age					
Analysis	Comment	U (ppm)	Th (ppm)	Pb (ppm)	Th/U	f206 (%)[a]	$^{207}Pb/^{235}U$	±1σ (%)	$^{206}Pb/^{238}U$	±1σ (%)	Rho	$^{207}Pb/^{206}Pb$	±1σ (%)	Conc. %[b]	$^{207}Pb/^{206}Pb$	±1σ	$^{206}Pb–^{238}U$	±1σ	207 Corr.[c]	±1σ
Pegmatite SVL 144																				
n3407–1r1	High common Pb	8735	147	[543]	0.017	77.82	0.15702	13.40	0.0239	0.92	0.06902	0.04768	13.37	17	83.6	289.8	152.1	1.4	152.4	67.3
n3407–4r	Intermediate common Pb	797	3	[94]	0.004	2.79	0.92196	2.20	0.1066	0.96	0.43628	0.06274	1.98	107	699.3	41.6	652.9	6.0	651.8	6.7
n3407–11r	High common Pb	4208	49	[241]	0.012	20.72	0.31202	16.62	0.0389	1.73	0.10384	0.05822	16.53	155	537.9	325.7	245.8	4.2	243.6	9.4
n3407–12r	High common Pb	6268	83	152	0.013	5.97	0.19824	38.35	0.0219	2.59	0.06758	0.06555	38.26	183	792.0	646.8	139.9	3.6	136.9	4.9
n3407–13r	High common Pb	2660	21	[244]	0.008	4.98	0.66756	4.24	0.0790	0.99	0.23322	0.06125	4.12	125	648.2	86.1	490.4	4.7	487.8	6.0
n3407–14cr	Low common Pb	1825	12	212	0.006	0.53	0.92535	1.18	0.1092	0.96	0.81446	0.06145	0.68	98	655.0	14.6	668.2	6.1	668.5	6.3
n3407–15r	High common Pb	4086	42	[253]	0.010	4.98	0.42327	2.88	0.0537	0.93	0.32273	0.05718	2.73	133	498.3	59.0	337.1	3.1	335.5	4.0
n3407–16c	High common Pb	6977	73	[437]	0.010	13.28	0.37866	5.09	0.0472	1.04	0.20538	0.05819	4.98	146	536.9	105.3	297.3	3.0	295.1	6.8
n3407–16cr	High common Pb	2486	27	[347]	0.011	30.24	0.64142	10.63	0.0836	0.97	0.09077	0.05565	10.59	81	438.5	219.8	517.5	4.8	518.8	28.6
n3407–17r	Intermediate common Pb	2842	12	[228]	0.004	3.04	0.59526	1.98	0.0716	1.73	0.87605	0.06034	0.95	129	615.7	20.5	445.5	7.5	443.0	7.8
n3407–18r	High common Pb	1962	35	[243]	0.018	38.24	0.57461	47.21	0.0677	2.64	0.05582	0.06157	47.13	137	659.2	778.8	422.2	10.8	418.8	35.4
n3407–19cr	Low common Pb; Rev. Dis.	2380	16	299	0.007	0.39	1.01039	1.05	0.1181	0.97	0.92184	0.06205	0.41	93	675.9	8.7	719.6	6.6	720.7	6.8
n3407–20cr	Low common Pb	4389	33	211	0.007	0.50	0.36514	1.20	0.0455	1.01	0.84764	0.05826	0.63	148	539.6	13.8	286.6	2.8	284.3	2.9
n3407–21r	High common Pb	4819	39	[275]	0.008	11.46	0.34593	32.07	0.0453	1.79	0.05588	0.05541	32.02	134	428.7	589.5	285.5	5.0	284.3	7.1
n3407–22r	Intermediate common Pb	2965	30	170	0.010	3.82	0.44794	1.66	0.0540	1.15	0.69290	0.06020	1.20	146	610.8	25.7	338.8	3.8	335.9	4.3
n3407–23c	High common Pb	786	8	83	0.010	12.85	0.85702	7.63	0.0990	0.93	0.12216	0.06279	7.57	114	701.0	153.5	608.5	5.4	606.5	13.0
n3407–24r	High common Pb	4316	39	[292]	0.009	6.24	0.45675	3.27	0.0572	0.94	0.28794	0.05794	3.13	133	527.7	67.1	358.4	3.3	356.5	4.6
n3407–25cr	Low common Pb; Rev. Dis.	2506	8	322	0.003	0.23	1.02787	0.97	0.1210	0.92	0.95187	0.06160	0.30	88	660.1	6.4	736.5	6.4	738.6	6.6
n3407–26r	High common Pb	2595	47	[319]	0.018	21.14	0.69982	8.38	0.0821	0.95	0.11290	0.06182	8.33	125	668.0	169.0	508.6	4.6	505.8	18.3
n3407–27r	High common Pb	5122	82	[294]	0.016	26.17	0.28705	15.23	0.0364	0.95	0.06237	0.05722	15.20	155	500.1	303.8	230.4	2.2	228.5	10.9
n3407–28r	Intermediate common Pb	4511	46	[157]	0.010	3.04	0.23241	4.89	0.0314	0.93	0.19074	0.05370	4.80	145	358.5	104.8	199.2	1.8	198.3	2.1
n3407–29r	High common Pb	7260	59	[266]	0.008	15.77	0.16726	16.39	0.0275	1.09	0.06679	0.04412	16.35	– 172	– 103.7	359.8	174.8	1.9	176.0	4.4

Table 1. Continued.

Analysis	Comment	U (ppm)	Th (ppm)	Pb (ppm)	Th/U	f206 (%)[a]	Ratios $^{207}Pb/^{235}U$	±1σ (%)	$^{206}Pb/^{238}U$	±1σ (%)	Rho	$^{207}Pb/^{206}Pb$	±1σ (%)	Conc. %[b]	Age $^{207}Pb/^{206}Pb$	±1σ ±1σ	$^{206}Pb–^{238}U$	±1σ	207 Corr.[c]	±1σ
Augen gneiss SVL145																				
n3408–1c	Zoned core – Mag.	263	166	53	0.63	{0.07}	1.56718	1.52	0.1598	1.16	0.76302	0.07111	0.98	101	960.5	19.9	955.9	10.3	955.7	10.8
n3408–2c	Zoned core – Mag.	395	270	81	0.69	{0.00}	1.57606	1.42	0.1615	1.19	0.84116	0.07079	0.77	98	951.4	15.6	964.9	10.7	965.5	11.2
n3408–2r	Bright rim – zoned core Mix	117	61	21	0.52	0.20	1.32893	2.08	0.1467	1.16	0.55840	0.06572	1.73	89	797.6	35.8	882.2	9.6	885.2	10.1
n3408–3c	Zoned dark core – Mag	612	120	105	0.20	0.13	1.51145	1.39	0.1530	1.20	0.86215	0.07163	0.70	106	975.5	14.3	918.0	10.3	915.7	10.7
n3408–3r	Bright rim	35	0	4	0.01	{0.18}	0.86465	3.07	0.1027	1.40	0.45547	0.06103	2.74	102	640.5	57.8	630.5	8.4	630.3	8.7
n3408–4c	Zoned inner core – Xen.	626	225	164	0.36	0.08	2.57226	1.62	0.2166	1.48	0.91232	0.08614	0.67	106	1341.3	12.8	1263.8	17.0	>1200	
n3408–4r1	Zoned dark inner rim – Mag.	319	50	56	0.16	0.07	1.53397	1.63	0.1583	1.44	0.88344	0.07028	0.76	99	936.6	15.5	947.3	12.7	947.7	13.2
n3408–4r2	Bright rim – zoned core Mix	501	16	70	0.03	0.08	1.22759	1.77	0.1303	1.62	0.91076	0.06831	0.73	111	878.0	15.1	789.8	12.0	787.0	12.4
n3408–5r1	Zoned dark inner rim – Mag.	563	64	100	0.11	0.03	1.55426	1.65	0.1598	1.47	0.89373	0.07053	0.74	99	944.0	15.0	955.8	13.1	956.2	13.6
n3408–5r2	Zoned dark inner rim – Mag.	264	95	50	0.36	{0.04}	1.58178	1.82	0.1590	1.55	0.85425	0.07216	0.95	104	990.6	19.1	951.1	13.7	949.4	14.3
n3408–5r3	Zoned core – Mag.	190	69	36	0.36	{0.04}	1.55791	1.89	0.1588	1.55	0.82072	0.07115	1.08	101	961.8	21.9	950.1	13.7	949.6	14.3
n3408–6c	Zoned core – Mag.	203	100	39	0.49	{0.05}	1.50970	1.68	0.1565	1.42	0.84618	0.06995	0.89	99	926.9	18.3	937.5	12.4	937.9	12.9
n3408–6r1	Zoned dark inner rim – Mag.	126	51	23	0.40	{0.09}	1.51203	1.86	0.1563	1.48	0.79469	0.07017	1.13	100	933.4	23.0	936.1	12.9	936.2	13.4
n3408–6r2	Zoned dark inner rim – Mag.	613	69	106	0.11	0.06	1.51578	1.61	0.1558	1.49	0.92557	0.07058	0.61	101	945.3	12.4	933.2	12.9	932.7	13.4
n3408–6r3	Bright rim	69	1	8	0.02	{0.17}	0.88304	2.66	0.1026	1.38	0.51974	0.06240	2.28	109	687.9	47.8	629.8	8.3	628.5	8.6
n3408–7c	Zoned dark core – Mag.	975	554	185	0.57	0.33	1.50200	1.52	0.1544	1.40	0.92383	0.07055	0.58	102	944.4	11.9	925.6	12.1	924.9	12.6
n3408–7r1	Zoned dark inner rim – Mag.	500	54	87	0.11	0.03	1.54459	1.57	0.1581	1.44	0.91716	0.07084	0.63	101	952.9	12.8	946.4	12.7	946.1	13.2
n3408–8c	Zoned core – Mag.	247	174	50	0.71	{0.05}	1.52909	1.66	0.1578	1.43	0.86229	0.07029	0.84	99	937.0	17.2	944.3	12.6	944.6	13.1
n3408–8r1	Zoned dark inner rim – Mag.	444	165	84	0.37	{0.03}	1.56009	1.57	0.1603	1.44	0.92180	0.07057	0.61	98	944.8	12.4	958.7	12.9	959.3	13.4
n3408–9c	Zoned core – Mag.	202	178	43	0.88	{0.02}	1.53109	1.76	0.1579	1.41	0.80059	0.07034	1.05	99	938.3	21.4	944.9	12.4	945.2	12.9
n3408–9r1	Zoned dark inner rim – Mag.	494	54	84	0.11	0.05	1.51864	1.59	0.1555	1.39	0.87460	0.07085	0.77	102	953.1	15.7	931.5	12.0	930.6	12.5
n3408–9r2	Bright rim – Pb loss	36	1	4	0.02	{0.87}	0.96715	3.84	0.1001	1.60	0.41712	0.07010	3.49	136	931.4	70.0	614.7	9.4	607.1	9.7
n3408–10c	Zoned core – Mag.	225	202	48	0.89	{0.06}	1.57501	1.93	0.1589	1.41	0.73067	0.07188	1.32	103	982.5	26.6	950.8	12.5	949.4	13.0
n3408–10r1	Zoned dark inner rim – Mag.	316	79	58	0.25	{0.05}	1.54893	1.68	0.1598	1.38	0.82604	0.07031	0.94	98	937.4	19.2	955.5	12.3	956.3	12.9
n3408–10r2	Bright rim – zoned core Mix	211	60	35	0.29	0.23	1.38844	2.15	0.1457	1.38	0.64552	0.06914	1.64	103	902.8	33.4	876.5	11.4	875.6	11.8
n3408–11r1	Bright rim	36	0	4	0.00	{0.58}	0.91817	3.58	0.1051	1.50	0.42039	0.06336	3.24	111	720.2	67.4	644.3	9.2	642.5	9.6
n3408–12c	Zoned core – Mag.	400	6	70	0.02	{0.04}	1.59607	1.62	0.1632	1.43	0.88091	0.07095	0.77	98	956.0	15.6	974.3	12.9	975.1	13.5
n3408–12r1	Zoned dark inner rim – Mag.	289	23	52	0.08	{0.06}	1.64166	1.70	0.1648	1.39	0.81836	0.07224	0.98	101	992.8	19.8	983.4	12.7	983.0	13.3
n3408–12r2	Bright rim – Pb loss	70	4	9	0.05	{0.17}	1.16900	3.35	0.1167	3.01	0.89883	0.07262	1.47	131	1003.4	29.6	711.8	20.3	703.2	20.7
n3408–13c	Zoned core – Mag.	78	45	15	0.58	{0.00}	1.54297	2.67	0.1605	1.40	0.52436	0.06973	2.27	95	920.4	46.0	959.5	12.5	961.1	13.2
n3408–13r	Bright rim –Mixed?	35	1	4	0.02	{0.00}	0.96771	4.18	0.1134	1.39	0.33397	0.06190	3.94	97	670.7	82.0	692.4	9.2	692.9	9.6

Notes:
Abbreviations: Conc. = concordance; Mag = magmatic; Rev. Dis = Reversely discordant; Xe = xenocryst
a – f_{206} % is the percentage of common ^{206}Pb, estimated from the measured ^{204}Pb. Figures in parentheses indicate when no correction has been applied.
b – Conc. % is the % age discordance between $^{207}Pb–^{206}Pb$ and $^{206}Pb–^{238}U$ ages as defined = 100 – ([($^{238}U–^{206}Pb$ date) – ($^{207}Pb–^{206}Pb$ date)]/($^{207}Pb–^{206}Pb$ date) × 100).
c – 207-corrected ages calculated by projecting from an assumed common Pb composition ($^{207}Pb/^{206}Pb$ = 0.83) through the analysis onto Concordia (Ludwig, 2003).

tectonostratigraphical position (probably similar to the BIS's) from Oscar II Land, in the northern part of Svalbard's Southwestern Province. Thus, it is now evident that all three Svalbard provinces include magmatic units of similar early Tonian age, suggesting a common history at this time.

5.c. Late Cryogenian (Torellian) metamorphism, deformation and pegmatite generation

Zircons from the BIS pegmatite (SVL 144), yielding a discordia upper intercept age of 665 ± 11 Ma, and the zircon rims from augen gneiss (SVL 145) with an age of 635 ± 10 Ma both indicate the importance of a late Cryogenian tectonometamorphic event in Svalbard's Southwestern Province. Similar ages have been obtained from pegmatites in the Isbjørnhamna Group of southwestern Wedel Jarlsberg Land (Majka *et al.* 2012) where small, inclusion-rich, metamict zircons from the Skoddefjellet pegmatite yielded an ion microprobe age of *c.* 650 Ma and monazite and uraninite from the same pegmatite yielded slightly older 680–660 Ma U–Th–total Pb ages. Based on mineralogy, the Skoddefjellet pegmatite was classified as Muscovite–Rare Element type, Rare Earth Element subtype (Majka *et al.* 2012), which typically forms under moderate- to high-amphibolite-facies conditions (Černy & Ercit, 2005). The Isbjørnhamna Group host rocks for the Skoddefjellet pegmatite were subjected to Barrovian amphibolite-facies metamorphism (up to *c.* 11 kbar and 670 °C) at *c.* 645 Ma, which supports syn-metamorphic formation of the pegmatite. Similarly, the BIS pegmatite (SVL 144) could have been formed during the amphibolite-facies metamorphism of the host augen gneiss. The BIS augen gneisses contain metamorphic garnet, which suggests a metamorphism under at least moderate grade. Rare schists intercalated with the augen gneisses, and containing two generations of garnet, yielded preliminary minimum pressure–temperature (*P–T*) conditions, based on thermodynamic modelling of phase equilibria, of *c.* 550 °C and 6 kbar for an older metamorphic event (garnet-I) and *c.* 500 °C and 12 kbar for a younger one (garnet-II; Kośmińska *et al.* 2013). If the *P–T* conditions obtained from these schists are representative for the whole BIS, the zircon rims from the augen gneiss (SVL 145) may date an older amphibolite-facies event, rather than a high pressure – low temperature (HP–LT) event, but an unequivocal judgement is not possible with the current state of knowledge.

Regional metamorphism of the Isbjørnhamna Group at *c.* 640 Ma (Majka *et al.* 2008) has helped constrain the age of the Torellian Unconformity (Birkenmajer, 1975; Bjørnerud, 1990) and the timing of deformation of the underlying Deilegga Group metasedimentary formations. Dating of detrital monazite in the Deilegga and overlying Sofiebogen groups (Czerny *et al.* 2010), with 650 Ma grains in the latter and none in the former, have provided further support for this interpretation of the tectonothermal history and the importance of the Torellian Orogeny in Svalbard's Southwestern Province.

A late Cryogenian *c.* 660 Ma U–Pb zircon age has also been reported from Svalbard's Northwestern Province, from agmatites in the Richarddalen Complex (Peucat *et al.* 1989; Gromet & Gee, 1998). Somewhat younger (mainly Ediacaran) ages were obtained on hornblende from amphibolitized eclogites and hornblendic gneisses in this complex by the K–Ar method (Gee *in* Gayer *et al.* 1966) and subsequently by the Ar–Ar method (Dallmeyer, Peucat & Ohta, 1990), suggesting the possibility of late Neoproterozoic deformation and metamorphism. However, this interpretation did not find support in subsequent U–Pb titanite investigations (Gromet & Gee, 1998), which provided strong evidence for mid Ordovician (*c.* 455 Ma) eclogite-facies metamorphism.

The evidence that late Neoproterozoic tectonothermal events are more widespread in the Southwestern Province than hitherto recognized implies that the 'basement block', comprising the Eimfjellet–Isbjørnhamna units, is not exotic as previously suggested (Majka *et al.* 2008; Mazur *et al.* 2009) and the Vimsodden–Kosibapasset shear zone may not necessarily be a terrane boundary. Evidence from Wedel Jarlsberg Land suggests that the Torellian Orogeny is likely to have influenced much, if not most, of Svalbard's Southwestern Province. Caledonian metamorphism and deformation can be expected to have obscured the Neoproterozoic tectonothermal history, if the latter did not exceed greenschist facies.

5.d. Caledonian overprint

The lack of evidence of Caledonian influence on the zircons in both the BIS pegmatite and the augen gneiss indicates that Caledonian metamorphism probably did not exceed greenschist facies. Kośmińska *et al.* (2013) have reported HP–LT metamorphism following an amphibolite-facies event for schists occurring within the BIS. In this case, the HP–LT event may be of Caledonian age (*c.* 470 Ma), like in the Motalafjella region (Horsfield, 1972; Dallmeyer, Peucat & Ohta, 1990; Bernard-Griffiths, Peucat & Ohta, 1993), but it probably would not cause the growth of zircon. Dallman *et al.* (1990) reported K–Ar ages of micas clustering around 460 Ma for the lithologies belonging to the Magnethøgda sequence, hence probably to the BIS. These ages are similar to those known from the HP–LT units of the Vestgötabreen Complex in the Motalafjella region.

5.e. Cretaceous tectonothermal events

Most of the dated zircons from the BIS pegmatite (SVL 144) plot along a discordia line with a lower intercept at 106 +20/−21 Ma. Early Cretaceous (100–130 Ma) mafic volcanism is well represented on Svalbard and its surrounding areas (Barents Sea Igneous Province). We note that the lower intercept age is similar to the K–Ar age of a dolerite sill exposed only *c*. 500 m away from the pegmatite (103 ± 4 Ma; Birkenmajer *et al*. 2010). It is, therefore, likely that the Pb-loss event in the pegmatite zircons was associated with widespread Cretaceous magmatic activity and that this was facilitated by these zircons susceptibility of Pb loss, as attested by their high-U content and internal textures. Alternatively, the Pb loss could have been connected to the late metamorphic extensive fluid activity.

5.f. Regional correlations and implications for the relative positions of Baltica and Laurentia in the Neoproterozoic

Zircon dating of the BIS provides evidence of previously unrecognized Tonian crystalline basement within Svalbard's Southwestern Province and a subsequent late Neoproterozoic metamorphic event. Recently, several reconstructions of Rodinia and the Grenvillian–Sveconorwegian belt have been proposed. Based on the Rodinia reconstruction by Li *et al*. (2008), who placed Baltica and Scotland near southeastern Greenland, several authors (e.g. Pettersson, Pease & Frei, 2010) explained the existence of the Tonian basement on Svalbard by very long-distance strike-slip movements of terranes. Cawood *et al*. (2010) favoured an external (in relation to the Grenville–Sveconorwegian belt) early Neoproterozoic Valhalla orogeny, based on palaeomagnetic data. Lorenz *et al*. (2012) suggested a northern continuation of the Grenville–Sveconorwegian orogen, beneath the continental shelves of the North Atlantic, within the hinterland of the Caledonides, into the High Arctic. This reconstruction allows an *in situ* late Neoproterozoic tectonothermal reworking of the Tonian crystalline basement. This late Neoproterozoic (Torellian in Svalbard) event is approximately contemporaneous with the early stages of the Timanide Orogen (e.g. Andreichev, 1998; Lorenz *et al*. 2004); however, the continuation of the Timanian basement northwestwards from the Pechora basin, beneath the Barents Sea, is not well defined. In northernmost Norway, the NW-trending Timanides are truncated by the Caledonian deformation front. The correlation of southwestern Svalbard with the Timanides suggests that the Timanide Orogen continued from the northern Urals region through the Barents shelf to Svalbard's Southwestern Province prior to the Iapetus Ocean opening and then split into at least two parts during separation of Baltica and Laurentia in the Ediacaran. Signs of rifting related to the Iapetus opening may be found in the mafic magmatism occurring as dykes within the Deilegga Group and lava flows within the Sofiebogen Group (Czerny, 1999), which is closely associated with the (post-)Torellian unconformity. This postulated northwestern arm of the Timanide Orogen argues against the Cambrian rotational models of Baltica (e.g. Hartz & Torsvik 2002; Cawood *et al*. 2010).

According to Trettin (1987), Harland (1997), Gee & Tebenkov (2004) and Mazur *et al*. (2009), at least some parts of the Southwestern Province may be correlated with the basement of the Pearya Terrane (Northern Ellesmere Island). The Proterozoic succession there, though less well known than on Svalbard, appears to be similar, comprising Grenville-age crystalline basement and thick sedimentary sequences of conglomerates, carbonates, quartzites and diamictites of probable glacial origin. According to Trettin's (1987) and Estrada *et al*.'s (2003) descriptions of the Yelverton Bay area within the Pearya Terrane, the oldest rocks of that basement are deformed orthogneisses with subordinate amphibolites, quartzites, mica schists and marbles (their Succession 1). This unit is overlain by lower grade monotonous siliciclastic and carbonaceous metasediments with minor admixture of mafic metavolcanites (Succession 2, Unit W1) and further up section by siliciclastic and calcareous metasediments, diamictites and metavolcanites (Succession 2, Unit W2). Little is known about the age of the Pearyan sedimentary units. The lower boundary of Unit W1 is indicated by a *c*. 965 Ma U–Pb zircon age of the basement orthogneisses (S. J. Malone, unpub. Ph.D. thesis, Univ. Iowa, 2012) and the upper limit of Unit W2 is defined by the existence of Cambrian volcanic rocks and younger Palaeozoic cover. It is suggested here that the Pearyan Succession 1 may correlate with southwestern Svalbard's amphibolite-facies rocks (Isbjørnhamna Group, Eimfjellet Complex and BIS), and that units W1 and W2 of Pearyan Succession 2 are equivalents of the Deilagga and Sofiebogen groups, respectively. This interpretation is supported by similar rock types, especially the occurrence of diamictites and associated metabasalts. Notably, recent detrital zircon dating of Ordovician, Silurian and Devonian rocks from Pearya yielded 680–570 Ma ages, typical for the Southwestern Svalbard Province and the Timanides (Malone & McClelland, 2010; S. J. Malone, unpub. Ph.D. thesis, Univ. Iowa, 2012). However, a better understanding of both Pearya's and southwestern Svalbard's geology, and more isotopic and petrological work is needed to test this hypothesis. Nevertheless, already back in the 19th century, baron Nordenskiöld (1876) stated that 'Probably during the Glacial Period the west coast of Spitzbergen was the west coast, not merely of a large island, but of a considerable Arctic continent, which towards the south was connected with Scandinavia, and towards the east with continental Siberia'. It appears that there are several lines of evidence to, at least partly, support this brave statement.

6. Conclusions

(1) This study shows that the Berzeliuseggene Igneous Suite of Svalbard's Southwestern Province is of Tonian (*c*. 950 Ma) age and shares an early Neoproterozoic history with the other Caledonian basement provinces of Svalbard.

(2) Zircon rims in augen gneisses and zircon from pegmatite show that the Torellian orogenic event is more widespread than previously thought and probably extends throughout the length of the entire Southwestern Province.

https://doi.org/10.1017/S0016756813000794 Published online by Cambridge University Press

(3) Possible correlation of Svalbard's Southwestern Province with the Timanides and the Pearya Terrane suggest that the late Neoproterozoic, post-Grenvillian and pre-Iapetian orogenic belt may have continued from northeastern Baltica to northern Laurentia.

Acknowledgements. We named the rocks described in this paper after Jacob Berzelius, a graduate of Uppsala University where J.M. and D.G.G. are affiliated. Marcia Bjørnerud, Maciek Dwornik and Nikolay Kuznetsov are thanked for their help during the fieldwork. Jurek Różański and his yacht Eltanin are thanked for their help during the transportation in Svalbard. Karolina Kośmińska is thanked for her help with technical preparation of the manuscript. She is also acknowledged for pointing out Nordenskiöld's publications from the 19th century. We thank Tom Moore and an anonymous reviewer for their constructive reviews. The study was supported by Ymer-80 Stiftelsen grant to J.M. and by a Polish Ministry of Science and Higher Education research grant N30704231/3336 to J.C. This paper is published with the permission of the Geological Survey of Denmark and Greenland. SIMS data was collected at the Nordsim facility, which is funded by the research councils of Denmark, Norway, Sweden, the Geological Survey of Finland and the Swedish Museum of Natural History. This is Nordsim Publication no. 351.

References

ANDREICHEV, V. L. 1998. *Isotope Geochronology of Intrusive Magmatism in the Northern Timans*. Ekaterinburg: Russian Academy of Sciences – Ural Division, 89 pp. (in Russian).

ARMSTRONG, H. A., NAKREM, H. A. & OHTA, Y. 1986. Ordovician conodonts from the Bulltinden Formation, Motalafjella, central-western Spitsbergen. *Polar Research* **4**, 17–23.

BALASHOV, Y. A., TEBENKOV, A. M., OHTA, Y., LARIONOV, A. N., SIROTKIN, A. N., GANNIBAL, L. F. & RYUNGENEN, G. I. 1995. Grenvillian U-Pb zircon ages of quartz porphyry and rhyolite clasts in a metaconglomerate at Vimsodden, southern Spitsbergen. *Polar Research* **14**, 291–302.

BALASHOV, Y. A., TEBENKOV, A. M., PEUCAT, J. J., OHTA, Y., LARIONOV, A. N. & SIROTKIN, A. N. 1996. Rb-Sr whole rock and U-Pb zircon dating of the granitic-gabbroic rocks from the Skålfjellet Subgroup, southwest Spitsbergen. *Polar Research* **15**, 167–81.

BERNARD-GRIFFITHS, J., PEUCAT, J. J. & OHTA, Y. 1993. Age and nature of protoliths in the Caledonian blueschist-eclogite complex of western Spitsbergen: a combined approach using U-Pb, Sm-Nd and REE whole-rock systems. *Lithos* **30**, 81–90.

BIRKENMAJER, K. 1975. Caledonides of Svalbard and plate tectonics. *Bulletin of the Geological Society of Denmark* **24**, 1–19.

BIRKENMAJER, K. 1990. *Geology of the Hornsund Area, Spitsbergen. Geological Map 1:75000, with Explanations*. Polish Academy of Sciences, Committee on Polar Research and Silesian University, 44 pp.

BIRKENMAJER, K. 2002. The Magnethøgda sequence (Hecla Hoek Succession), NW Torell Land, Spitsbergen: a revision of lithostratigraphy and age. *Bulletin Polish Academy of Sciences: Earth Sciences* **50**, 175–91.

BIRKENMAJER, K. 2010. The Kapp Lyell diamictites (Upper Proterozoic) at Bellsund, Spitsbergen: rock-sequence, sedimentological features, paleoenvironment. *Studia Geologica Polonica* **133**, 7–50.

BIRKENMAJER, K., KRAJEWSKI, K. P., PÉCSKAY, Z. & LORENC, M. W. 2010. K-Ar dating of basic intrusions at Bellsund, Spitsbergen, Svalbard. *Polish Polar Research* **31**, 2–16.

BJØRNERUD, M. 1990. Upper Proterozoic unconformity in northern Wedel-Jarlsberg Land, southwest Spitsbergen: lithostratigraphy and tectonic implications. *Polar Research* **8**, 127–40.

BJØRNERUD, M. 2010. Stratigraphic record of Neoproterozoic ice sheet collapse: the Kapp Lyell diamictite sequence, SW Spitsbergen, Svalbard. *Geological Magazine* **147**, 380–90.

CAWOOD, P. A., STRACHAN, R., CUTTS, K., KINNY, P. D., HAND, M. & PISAREVSKY, S. 2010. Neoproterozoic orogeny along the margin of Rodinia: Valhalla orogen, North Atlantic. *Geology* **38**, 99–102.

ČERNY, P. & ERCIT, T. S. 2005. The classification of granitic pegmatites revisited. *Canadian Mineralogist* **43**, 2005–26.

CORFU, F., HANCHAR, J. M., HOSKIN, P. W. O. & KINNY, P. 2003. Atlas of zircon textures. In *Zircon* (eds J. M. Hanchar & P. W. O. Hoskin), pp. 469–500. Reviews in Mineralogy and Geochemistry no. 53.

CZERNY, J. 1999. Petrogenesis of metavolcanites of the southern part of Wedel Jarlsberg Land (Spitsbergen). *Mineralogical Transactions* **86**, 88 pp.

CZERNY, J., KIERES, A., MANECKI, M., & RAJCHEL, J. 1993. *Geological Map of the SW Part of Wedel Jarlsberg Land, Spitsbergen 1:25000* (ed. A. Manecki). Cracow: Institute of Geology and Mineral Deposits, 61 pp.

CZERNY, J., MAJKA, J., GEE, D. G., MANECKI, M. & MANECKI, A. 2010. Torellian Orogeny: evidence of a Late Proterozoic tectonothermal event in southwestern Svalbard's Caledonian basement. *NGF Abstracts and Proceedings*, 35–36.

DALLMANN, W. K., HJELLE, A., OHTA, Y., SALVIGSEN, O., MAHER, H. D., BJØRNERUD, M., HAUSER, E. C. & CRADDOCK, C. 1990. *Geological Map of Svalbard 1:100,000, B11G Van Keulenfjorden*. Norsk Polarinstitutt Temakart No. 15, 58 pp.

DALLMEYER, R. D., PEUCAT, J. J. & OHTA, Y. 1990. Tectonothermal evolution of contrasting metamorphic complexes in northwestern Spitsbergen (Biskayerhalvøya): evidence from 40Ar/39Ar and Rb-Sr mineral ages. *Geological Society of America Bulletin* **102**, 653–63.

ESTRADA, S., PIEPJOHN, K., HENJES-KUNST, F. & VON GOSEN, W. 2003. Geology, magmatism, and structural evolution of the Yelverton Bay area, northern Ellesmere Island, Arctic Canada. *Polarforschung* **73**, 59–75.

FREI, D. & GERDES, A. 2009. Precise and accurate in situ U–Pb dating of zircon with high sample throughput by automated LA-SF-ICPMS. *Chemical Geology* **261**, 261–70.

GASSER, D. & ANDRESEN, A. 2013. Caledonian terrane amalgamation of Svalbard: detrital zircon provenance of Mesoproterozoic to Carboniferous strata from Oscar II Land, western Spitsbergen. *Geological Magazine*, published online 4 June 2013. doi: 10.1017/S0016756813000174.

GAYER, R. A., GEE, D. G., HARLAND, W. B., MILLER, J. A., SPALL, H. R., WALLIS, R. H. & WINSNES, T. S. 1966. Radiometric age determinations on rocks from Spitsbergen. *Norsk Polarinstitutt Skrifter* **137**, 1–39.

GEE, D. G. 1966. A note on the occurrence of eclogites in Spitsbergen. *Norsk Polarinstitutt Årbok* **1964**, 240–41.

GEE, D. G., BJÖRKLUND, L. & STØLEN, L. K. 1994. Early Proterozoic basement in Ny Friesland – implications for the Caledonian tectonics of Svalbard. *Tectonophysics* **231**, 171–82.

GEE, D. G. & HJELLE, A. 1966. On the crystalline rocks of northwest Spitsbergen. *Norsk Polarinstitutt Årbok* **1964**, 31–45.

GEE, D. G., JOHANSSON, Å., OHTA, Y., TEBENKOV, A. M., KRASILŠČHIKOV, A. A., BALASHOV, Y. A., LARIONOV, A. N., GANNIBAL, L. F. & RYUNGENEN, G. I. 1995. Grenvillian basement and a major unconformity within the Caledonides of Nordaustlandet, Svalbard. *Precambrian Research* **70**, 215–34.

GEE, D. G. & TEBENKOV, A. M. 1996. Two major unconformities beneath the Neoproterozoic Murchinsonfjorden Supergroup in the Caledonides of central Nordaustlandet, Svalbard. *Polar Research* **15**, 81–91.

GEE, D. G. & TEBENKOV, A. M. 2004. Svalbard: a fragment of the Laurentian margin. In *The Neoproterozoic Timanide Orogen of Eastern Baltica* (eds D. G. Gee & V. Pease), pp. 191–206. Geological Society of London, Memoirs no. 30.

GERDES, A. & ZEH, A. 2006. Combined U–Pb and Hf isotope LA-(MC)-ICP-MS analyses of detrital zircons: comparison with SHRIMP and new constraints for the provenance and age of an Armorican metasediment in Central Germany. *Earth and Planetary Science Letters* **249**, 47–61.

GROMET, L. P. & GEE, D. G. 1998. An evaluation of the age of high-grade metamorphism in the Caledonides of Biskayerhalvøya. *GFF* **120**, 199–208.

HARLAND, W. B. 1997. *The Geology of Svalbard*. Geological Society of London, Memoirs no. 17, 521 pp.

HARLAND, W. B., HAMBRY, M. J. & WADDAMS, P. 1993. The Vendian geology of Svalbard. *Norsk Polarinstitutt Skrifter* **193**, 1–130.

HARTZ, E. H. & TORSVIK, T. H. 2002. Baltica upside-down: a new plate tectonic model for Rodinia and the Iapetus Ocean. *Geology* **30**, 255–58.

HELLMAN, F. J., GEE, D. G., JOHANSSON, Å. & WITT-NILSSON, P. 1997. Single-grain Pb-evaporation geochronology constraints basement-cover relationships in the Lower Hecla Hoek Complex of northern Ny Friesland, Svalbard. *Chemical Geology* **137**, 117–34.

HELLMAN, F. J., GEE, D. G. & WITT-NILSSON, P. 2001. Late Archean basement in the Bangenhuken Complex of the Nordbreen Nappe, western Ny Friesland, Svalbard. *Polar Research* **20**, 49–59.

HORSFIELD, W. T. 1972. Glaucophane schists of Caledonian age from Spitsbergen. *Geological Magazine* **109**, 29–36.

JOHANSSON, Å., GEE, D. G., LARIONOV, A. N., OHTA, Y. & TEBENKOV, A. M. 2005. Grenvillian and Caledonian evolution of eastern Svalbard – a tale of two orogenies. *Terra Nova* **17**, 317–25.

JOHANSSON, Å., LARIONOV, A. N., TEBENKOV, A. M., GEE, D. G., WHITEHOUSE, M. J. & VESTIN, J. 2000. Grenvillian magmatism of western and central Nordaustlandet, northeastern Svalbard. *Transactions of the Royal Society of Edinburgh: Earth Sciences* **90**, 221–54.

KANAT, L. & MORRIS, A. 1988. A working stratigraphy for central western Oscar II Land, Spitsbergen. *Norsk Polarinstitutt Skrifter* **190**, 1–25.

KOŚMIŃSKA, K., MAJKA, J., KLONOWSKA, I., KRUMBHOLZ, M., MANECKI, M. & CZERNY, J. 2013. New blueschist facies province in the Caledonides of Svalbard. *Geophysical Research Abstracts* **15**, EGU2013-399.

LARIONOV, A. N. & TEBENKOV, A. M. 2004. New SHRIMP-II U-Pb zircon age data from granitic boulders in Vendian tillites of southern coast of Isfjorden, West Spitsbergen. Arctic geology, hydrocarbon resources and environmental challenges. *Abstracts and Proceedings of the Geological Society of Norway, NGF* **2**, 88–9.

LARIONOV, A. N., TEBENKOV, A. M., GEE, D. G., CZERNY, J. & MAJKA, J. 2010. Recognition of Precambrian tectonostratigraphy in Wedel-Jarlsberg Land, southwestern Spitsbergen. *Abstracts and Proceedings of the Geological Society of Norway, NGF* **1**, 106 pp.

LI, Z. X., BOGDANOVA, S. V., COLLINS, A. S., DAVIDSON, A., DE WAELE, B., ERNST, R. E., FITZSIMONS, I. C. W., FUCK, R. A., GLADKOCHUB, D. P., JACOBS, J., KARLSTROM, K. E., LU, S., NATAPOV, L. M., PEASE, V., PISAREVSKY, S. A., THRANE, K. & VERNIKOVSKY, V. 2008. Assembly, configuration, and break-up history of Rodinia: a synthesis. *Precambrian Research* **160**, 179–210.

LORENZ, H., GEE, D. G., LARIONOV, A. N. & MAJKA, J. 2012. The Grenville–Sveconorwegian orogen in the high Arctic. *Geological Magazine* **149**, 875–91.

LORENZ, H., PYSTIN, A. M., OLOVYANISHNIKOV, V. G. & GEE, D. G. 2004. Neoproterozoic high-grade metamorphism of the Kanin Peninsula, Timanide Orogen, northern Russia. In *The Neoproterozoic Timanide Orogen of Eastern Baltica* (eds D. G. Gee & V. Pease), pp. 59–68. Geological Society of London, Memoir, no. 30.

LUDWIG, K. R. 2003. *User's Manual for Isoplot 3.00 a Geochronological Toolkit for Microsoft Excel*. Berkeley Geochronology Center Special Publication no. 4.

MAJKA, J., CZERNY, J., LARIONOV, A. N., PRŠEK, J. & GEE, D. G. 2012. Neoproterozoic pegmatite from Skoddefellet, Wedel Jarlsberg Land, Spitsbergen: additional evidence for c. 640Ma tectonothermal event in the Caledonides of Svalbard. *Polish Polar Research* **33**, 1–17.

MAJKA, J., LADENBERGER, A. & KUZNETSOV, N. 2009. Crustal growth and crustal recycling in the Neoproterozoic Torellian Orogen, SW Svalbard: U/Pb zircon geochronology and Hf isotopic characteristics. *Mineralogia – Special Papers* **35**, 98.

MAJKA, J., MAZUR, S., MANECKI, M., CZERNY, J. & HOLM, D. 2008. Late Neoproterozoic amphibolite facies metamorphism of a pre-Caledonian basement block in southwest Wedel Jarlsberg Land, Spitsbergen: new evidence from U-Th-Pb dating of monazite. *Geological Magazine* **145**, 822–30.

MAJOR, H. & WINSNES, T. S. 1955. Cambrian and Ordovician fossils from Sørkapp Land, Spitsbergen. *Norsk Polarinstitutt Skrifter* **106**, 1–47.

MALONE, S. J. & MCCLELLAND, W. C. 2010. Detrital zircon geochronology of Neoproterozoic and Paleozoic units of the Pearya Terrane, Ellesmere Island, Canada. *Geological Society of America Meeting*, paper no. 243–3.

MANECKI, M., HOLM, D. K., CZERNY, J. & LUX, D. 1998. Thermochronological evidence for late Proterozoic (Vendian) cooling in southwest Wedel Jarlsberg Land, Spitsbergen. *Geological Magazine* **135**, 63–9.

MARTIN, L. A. J., DUCHÊNE, S., DELOULE, E. & VANDERHAEGH, O. 2008. Mobility of trace elements and oxygen in zircon during metamorphism: consequences for geochemical tracing. *Earth and Planetary Science Letters* **267**, 161–74.

MATTINSON, J. M. 2010. Analysis of the relative decay constants of 235U and 238U by multi-step CA-TIMS measurements of closed-system natural zircon samples. *Chemical Geology* **275**, 186–98.

MAZUR, S., CZERNY, J., MAJKA, J., MANECKI, M., HOLM, D. K., SMYRAK, A. & WYPYCH, A. 2009. A strike-slip terrane boundary in Wedel Jarlsberg Land, Svalbard, and its bearing on correlations of SW Spitsbergen with the Pearya terrane and Timanide belt. *Journal of the Geological Society, London* **166**, 529–44.

McLaren, A. C., Fitzgerald, J. D. & Williams, I. S. 1994. The microstructure of zircon and its influence on the age determination from Pb/U isotopic ratios measured by ion microprobe. *Geochimica et Cosmochimica Acta* **58**, 993–1005.

Myhre, P. I., Corfu, F. & Andresen, A. 2009. Caledonian anatexis of Grenvillian crust: a U/Pb study of Albert I Land, NW Svalbard. *Norwegian Journal of Geology* **89**, 173–91.

Nasdala, L., Hofmeister, W., Norberg, N., Mattinson, J. M., Corfu, F., Dörr, W., Kamo, S. L., Kennedy, A. K., Kronz, A., Reiners, P. W., Frei, D., Košler, J., Wan, Y., Götze, J., Häger, T., Kröner, A. & Valley, J. W. 2008. Zircon M257 – a homogeneous natural reference material for the ion microprobe U-Pb analysis of zircon. *Geostandards and Geoanalytical Research* **32**, 247–65.

Nordenskiöld, A. E 1876. Sketch of the geology of Ice Sound and Bell Sound, Spitzbergen. *Geological Magazine* (Decade 2) **3**, 16–23.

Ohta, Y. 1982. Lithostratigraphy of the Hecla Hoek rocks in central Nordaustlandet and their relationships to the Caledonian granitic-migmatitic rocks. *Norsk Polarinstitutt Skrifter* **178**, 41–60.

Ohta, Y. 1985. Geochemistry of Precambrian basic igneous rocks between St. Jonsfjorden and Isfjorden, central western Spitsbergen, Svalbard. *Polar Research* **3**, 49–67.

Ohta, Y. & Larionov, A. M. 1998. Grenvillian single grain zircon Pb age of granitic rock from the southern island of Hesteskoholmen, Liefdefjorden, NW Spitsbergen. *Polar Research* **17**, 147–54.

Ohta, Y., Larionov, A. N. & Tebenkov, A. M. 2003. Single-grain zircon dating of the metamorphic and granitic rocks from the Biscayarhalvøya-Holtedahlfonna zone, north-west Spitsbergen. *Polar Research* **22**, 247–65.

Ohta, Y., Larionov, A. N., Tebenkov, A. M., Lepvrier, C., Maluski, H., Lange, M. & Hellibrant, B. 2002. Single zircon Pb-evaporation and 40Ar/39Ar dating of the metamorphic and granitic rocks in north-west Spitsbergen. *Polar Research* **21**, 73–89.

Pettersson, C. H., Pease, V. & Frei, D. 2009. U-Pb zircon provenance of metasedimentary basement of the Northwestern Terrane, Svalbard: Implications for the Grenvillian-Sveconorwegian orogeny and development of Rodinia. *Precambrian Research* **175**, 206–20.

Pettersson, C. H., Pease, V. & Frei, D. 2010. Detrital zircon U-Pb ages of Silurian-Devonian sediments from NW Svalbard: a fragment of Avalonia and Laurentia? *Journal of the Geological Society, London* **167**, 1019–32.

Pettersson, C. H., Tebenkov, A. M., Larionov, A. N., Andresen, A. & Pease, V. 2009. Timing of migmatization and granite genesis in the Northwestern Terrane of Svalbard, Norway: implications for regional correlations in the Arctic Caledonides. *Journal of the Geological Society, London* **166**, 147–58.

Peucat, J. J., Ohta, Y., Gee, D. G. & Bernard-Griffiths, J. 1989. U-Pb, Sr, and Nd evidence for Grenvillian and latest Proterozoic tectonothermal activity in the Spitsbergen Caledonides, Arctic Ocean. *Lithos* **22**, 275–85.

Piepjohn, K., Thiedig, F. & Manby, G. M. 2001. Nappe stacking on Brøggerhalvøya, NW Spitsbergen. In *Intra-Continental Fold Belts CASE 1 West Spitsbergen* (ed. F. Tessensohned), pp. 83–108. Geologisches Jahrbuch, Polar Issue no. 7.

Scrutton, C. T., Horsfield, W. T. & Harland, W. B. 1976. Silurian fossils from western Spitsbergen. *Geological Magazine* **113**, 519–23.

Sláma, J., Košler, J., Condon, D. J., Crowley, J. L., Gerdes, A., Hanchar, J. M., Horstwood, M. S. A., Morris, G. A., Nasdala, L., Norberg, N., Schaltegger, U., Schoene, B., Tubrett, M. N. & Whitehouse, M. J. 2008. Plešovice zircon – a new natural reference material for U–Pb and Hf isotopic microanalysis. *Chemical Geology* **249**, 1–35.

Smith, M. P. 2000. Cambro-Ordovician stratigraphy of Bjørnøya and North Greenland: constraints on tectonic models for the Arctic Caledonides and the Tertiary opening of the Greenland Sea. *Journal of the Geological Society, London* **157**, 459–70.

Stacey, J. S. & Kramers, J. D. 1975. Approximation of terrestrial lead isotope evolution by a 2-stage model. *Earth and Planetary Science Letters* **26**, 207–21.

Steiger, R. H. & Jäger, E. 1977. Subcommission on geochronology: convention of the use of decay constants in geo- and cosmo-chronology. *Earth and Planetary Science Letters* **36**, 359–62.

Tebenkov, A. 1983. Late Precambrian magmatic formations of Nordaustlandet. In *Geologiya Spitsbergena: sbornik nauchnych trudov (The Geology of Spitsbergen: a collection of papers)* (eds A. A. Krasilshikov & V. A. Basovs), pp. 74–86. Leningrad: Sevmorgeo (in Russian).

Tebenkov, A., Sandelin, , S. Gee, D. G. & Johansson, Å. 2002. Caledonian migmatization in central Nordaustlandet, Svalbard. *Norsk Geologisk Tidskrift* **82**, 15–28.

Trettin, H. P. 1987. Pearya: a composite terrane with Caledonian affinities in northern Ellesmere Island. *Canadian Journal of Earth Sciences* **24**, 224–45.

Whitehouse, M. J., Kamber, B. & Moorbath, S. 1999. Age significance of U-Th-Pb zircon data from early Archean rocks of west Greenland – a reassessment based on combined ion-microprobe and imaging studies. *Chemical Geology* **160**, 201–24.

Wiedenbeck, M. 1995. An example of reverse discordance during ion microprobe zircon dating: an artifact of enhanced ion yields from a radiogenic labile Pb. *Chemical Geology* **125**, 197–218.

Wiedenbeck, M., All'e, P., Corfu, F., Griffin, W., Meier, M., Oberli, F., von Quadt, A., Roddick, J. C. & Spiegel, W. 1995. Three natural zircon standards for U–Th–Pb, Lu–Hf, trace element and REE analysis. *Geostandards Newsletter* **19**, 1–23.

Witt-Nilsson, P., Gee, D. G. & Hellman, F. 1998. Tectonostratigraphy of the Caledonian Atomfjella Antiform of northern Ny Friesland, Svalbard. *Norsk Geologisk Tidsskrift* **78**, 67–80.

https://doi.org/10.1017/S0016756813000794 Published online by Cambridge University Press